STM JOURNALS

International Journal of
Pollution: Prevention & Control

Volume 1, Issue 1, 2023
DOI (Journal): 10.37591/IJPPC
(January–June)

https://journals.stmjournals.com/ijppc

Research IJPPC

Comparison of Different Models for the Remediation of Crude Oil Contaminated Clay and Swampy Soil Environment

E.P. Uku[1,*], B.B. Dumkhana[2]

Abstract

This research was carried out to compare different mathematical models for the determination of best practice or method for remediation of crude oil contaminated clay and swampy soil environment. The results obtained were utilized to calculate the highest specific rates, the disassociation constant, and the kinetic values in terms of first- and second-order kinetics. The use of the Lineweaver Buck plot was taken into consideration for the different reactors, and the maximum specific rate of substrate degradation and disassociation constant were evaluated and determined for both the powdered forms of the moringa seed shell, yeast, and NPK (nitrogen, phosphorus, potassium) in the swampy soil (Moringa olefara), and the elephant grass, yeast, and NPK in the swampy soil (Pennisetum purpureum). According to the research, crude oil degraded more quickly in reactors that contained a mixture of yeast, NPK, and powdered swamp soil (Moringa oleifera) from moringa seeds.

Keywords: Moringa seed, remediation, clay soil, swampy soil, comparison

INTRODUCTION

Bioremediation techniques are adaptable and can be used at various stages of treatment, according to research on the behavior of pollutants [1–3]. The concept's use improved decontamination of soils, sediments, surface water, and ground water, as well as the removal of pollutants from raw materials prior to processing and the treatment of waste and effluent streams before release. Ground water, soil lagoons, sludge, and process water streams can all be cleaned up using bioremediation techniques (including phytoremediation), which have a wide range of applications in environmental management. The quick clean-up activities are one of the most significant examples of large-scale remediation [4, 5].

MODEL COMPARISON

The First-Order Biodegradation Rate Kinetic Model

The first-order biodegradation rate kinetic model for prediction of total petroleum hydrocarbon (TPH) reduction was developed using the principle of mass conservation in a batch reactor [6]. A typical batch reactor is represented in Figure 1.

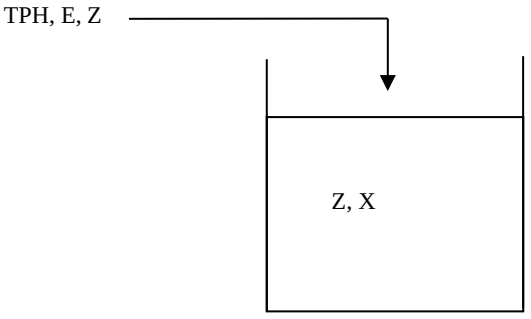

Figure 1. Batch reactor.

***Author for Correspondence**
E.P. Uku
E-mail: ukueruni@gmail.com

[1]Lecturer, Chemical Engineering Department, Federal University, Otuoke, Bayelsa State, Nigeria
[2]Lecturer, Agricultural and Environmental Engineering Department, Rivers State University, Port Harcourt, Rivers State, Nigeria.

Received Date: May 07, 2023
Accepted Date: May 12, 2023
Published Date: May 15, 2023

Citation: E.P. Uku, B.B. Dumkhana. Comparison of Different Models for the Remediation of Crude Oil Contaminated Clay and Swampy Soil Environment. International Journal of Pollution Prevention & Control. 2023; 1(1): 1–8p.

The principle of mass conservation is stated as

$$\text{Inflow of mass into system} = \text{Outflow of mass from system} + \text{Rate of degradation due to reaction} + \text{Rate of accumulation of mass within system} \quad (1)$$

$$TPH + E + Z \xrightarrow{k_s} P + E + Z \quad (2)$$

The degradation reaction that takes place in the reactor can be represented by Equation (2),

where

$TPH =$ total petroleum hydrocarbon (pollutant) (g)

$E =$ bacteria

$Z =$ soil (kg)

P = products

$k_d =$ Degradation rate constant (unit according to model used)

$$\text{Inflow of mass into system} = Q_o C_{TPH\,(o)} \quad (3)$$

$$\text{Outflow of mass from system} = QC_{TPH} \quad (4)$$

$$\text{Rate of TPH degradation} = -r_{TPH}V \quad (5)$$

$$\text{Rate of accumulation} = -\frac{d(C_{TPH}V)}{dt} \quad (6)$$

Combining Equations (3) through (6) gives

$$Q_o C_{TPH(o)} = QC_{TPH} - r_{TPH}V + \frac{d(C_{TPH}V)}{dt} \quad (7)$$

Since there is no flow of materials in a batch reactor, the inflow of mass into reactor is equivalent to the out flow of mass from reactor [7, 8].

Thus,

$$Q_o C_{TPH(o)} = QC_{TPH} = 0 \quad (8)$$

Also, for a batch process, volume of reactor (vessel) is constant hence, the accumulation term is

$$\frac{d(C_{TPH}V)}{dt} = V\frac{dC_{TPH}}{dt} \quad (9)$$

Therefore, Equation (3–7) reduces to

$$-r_{TPH}V = -V\frac{dC_{TPH}}{dt}$$

or $$-r_{TPH} = -\frac{dC_{TPH}}{dt} \tag{10}$$

Assuming that the degradation of TPH is described by first-order kinetics, we have

$$-r_{TPH} = -\frac{dC_{TPH}}{dt} = k_d C_{TPH} \tag{11}$$

where

Q_o = Inlet volumetric flow rate (kg/day)

Q = Outlet volumetric flow rate (kg/day)

$C_{TPH(o)}$ = Initial concentration of pollutant (TPH) (mg/kg)

C_{TPH} = Instantaneous concentration of pollutant (TPH) (mg/kg)

V = Volume of reactor (m^3)

r_{TPH} = Rate of TPH degradation (mg/kg.day)

k_d = TPH degradation rate constant (day^{-1})

t = Time of TPH degradation (day)

Integration of Equation (11) by the separation of variable method yields the following:

$$\int_{C_{TPH(o)}}^{C_{TPH(t)}} \frac{dC_{TPH}}{C_{TPH}} = -k_d \int_0^t dt \tag{12}$$

$$\ln\left(\frac{C_{TPH(t)}}{C_{TPH(o)}}\right) = -k_d t \tag{13}$$

$$\ln C_{TPH(t)} - \ln C_{TPH(o)} = -k_d t$$

$$\ln C_{TPH(t)} = \ln C_{TPH(o)} - k_d t \tag{14}$$

Equation (14) can be simply written as

$$\ln C_{(t)} = \ln C_o - k_d t \tag{15}$$

Equation (15) can be compared with the general linear equation of the form

$$y = mx + C \tag{16}$$

where;

$y = \ln C_{(t)}$

$x = t$

$m = k_d$

$C = \ln C_o$

A plot of $\ln C_{(t)}$ against *t* gives a linear (straight line) graph with slope equivalent to "k_d" and intercept equivalent to $\ln C_o$.

However, to obtain the instantaneous TPH concentration, exponential of both sides of Equation (15) is taken to give

$$C_{TPH(t)} = C_{TPH(o)} \exp(-k_1 t) \tag{17}$$

Equation (17) is the predictive first-order kinetic model for TPH reduction during the treatment process [8].

The Second-Order Biodegradation Rate Kinetic Model

The degradation rate of TPH would be further tested with the second-order rate kinetics, and it is expressed as:

$$-r_{TPH} = -\frac{dC}{dt} = k_d C^2 \tag{18}$$

Upon integration of Equation (18), we have the following:

$$\int_{C_o}^{C_t} C^{-2} dC = -\int_0^t k_d \, dt$$

$$\frac{1}{C_t} - \frac{1}{C_0} = k_d t \tag{19}$$

or

$$\frac{1}{C_t} = \frac{1}{C_0} + k_d t \tag{20}$$

where

C_0 and C_t are the initial concentration and concentration of TPH at any time, t; while k_d is the degradation rate constant for the second order [9].

A plot of $\frac{1}{C_t}$ against t will give slope as k_d and $\frac{1}{C_0}$ as intercept.

Rearranging Equation (20) with little manipulations gives the TPH predictive equation using the second-order kinetic model as:

$$C_{TPH(t)} = \frac{C_{TPH(0)t}}{1 + C_{TPH(0)} k_2 t} \tag{21}$$

The Michaelis-Menten Biodegradation Rate Model

Similarly, the degradation rate of TPH was tested with the Michaelis-Menten biodegradation rate, and it is expressed as:

$$r_{TPH} = \frac{\mu_{max} C_{TPH(t)}}{K_s + C_{TPH(t)}} \tag{22}$$

Upon linearization, Equation (22) becomes

$$-\frac{1}{r_{TPH}} = -\frac{dC_{TPH(t)}}{dt} = \frac{1}{\mu_{max}} + \frac{K_s}{\mu_{max}} \left(\frac{1}{C_{TPH(t)}} \right) \tag{23}$$

where: μ_{max} is the maximum specific degradation rate, $C_{TPH(t)}$ is TPH concentration with time *t*, and K_s is the degradation rate constant relating to Michaelis-Menten [10].

A plot of $\frac{1}{r_{TPH}}$ against $\frac{1}{C_{TPH(t)}}$ gives the slope as $\frac{K_s}{\mu_{max}}$ and the intercept at $\frac{1}{\mu_{max}}$.

RESULTS AND DISCUSSION

Comparison of Model Performance in TPH Prediction

To demonstrate the performance of the models predicting the content of TPH in soil with time, the TPH content recorded from the experimental analysis for swampy soil treated with different weights of moringa seed shell in powdered form, yeast and NPK (nitrogen, phosphorus, potassium) in swampy soil was compared with the first-order, second-order, and Michaelis-Menten degradation rate models as shown in Figures 2–6.

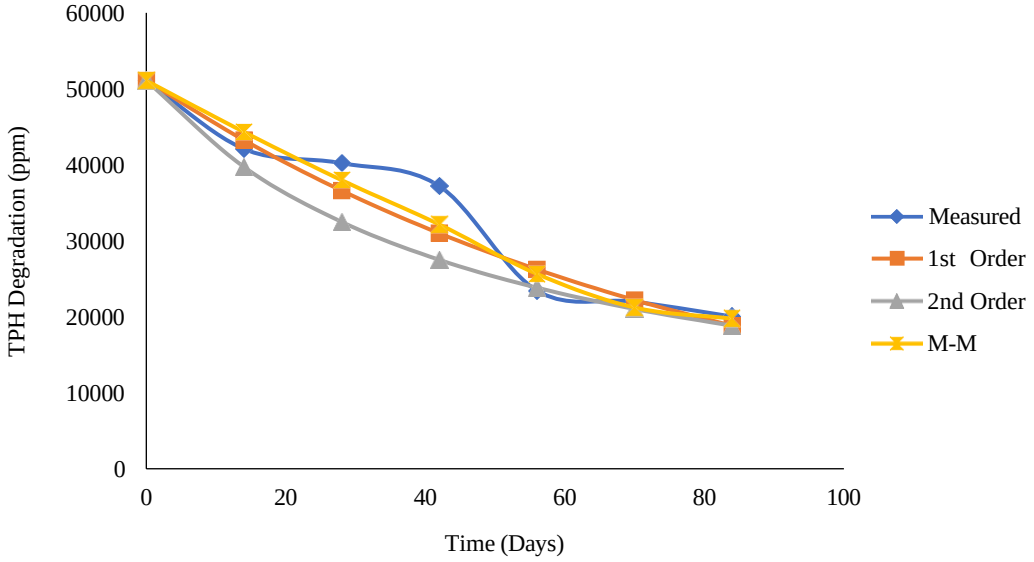

Figure 2. Comparison of models with 20 g moringa seed shell in powdered form, yeast and NPK (nitrogen, phosphorus, potassium) in swampy soil.

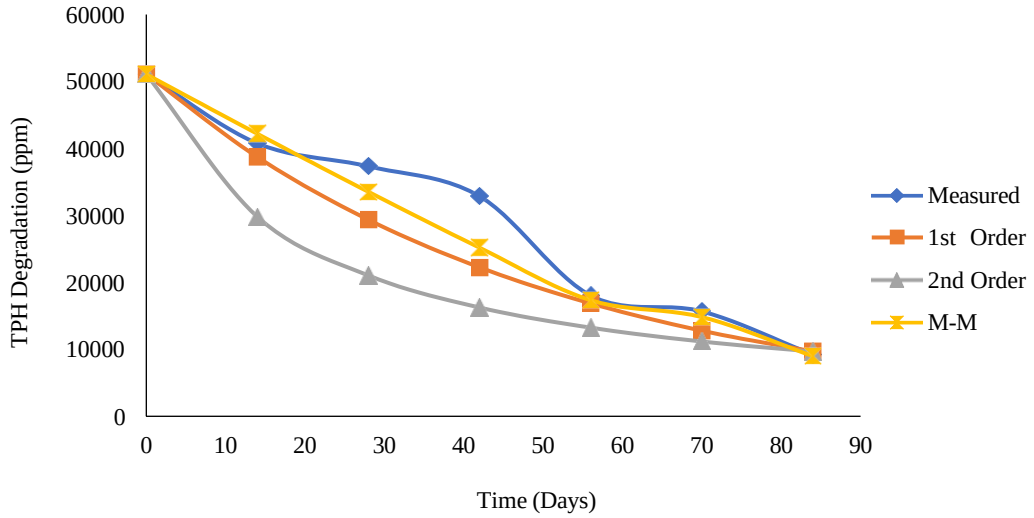

Figure 3. Comparison of models with 40 g moringa seed shell in powdered form, yeast and NPK (nitrogen, phosphorus, potassium) in swampy soil.

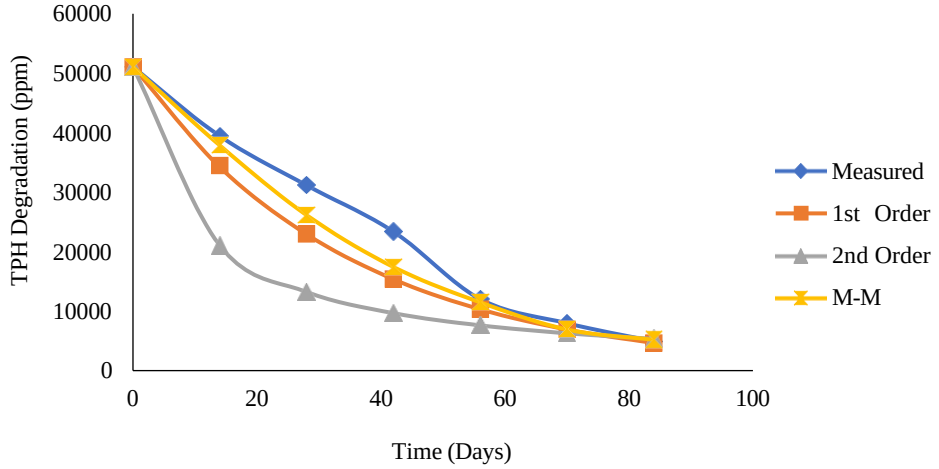

Figure 4. Comparison of models with 60 g moringa seed shell in powdered form, yeast and NPK (nitrogen, phosphorus, potassium) in swampy soil.

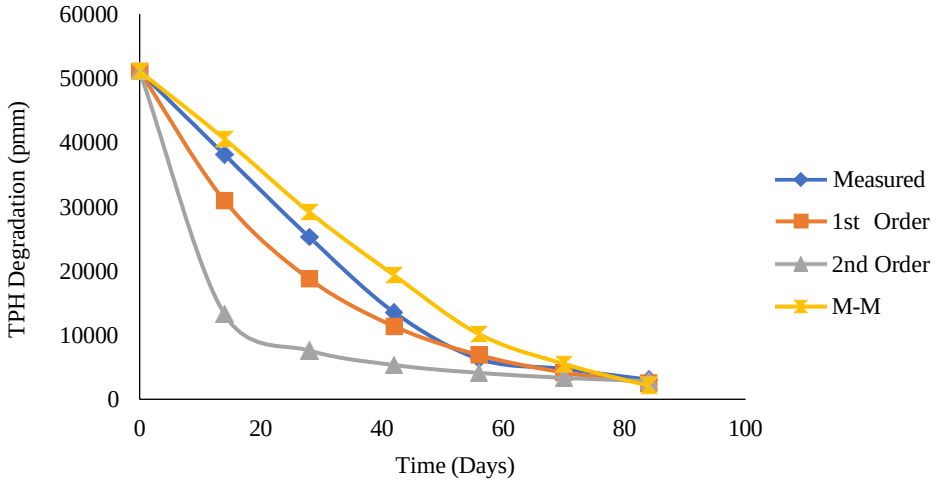

Figure 5. Comparison of models with 80 g moringa seed shell in powdered form, yeast and NPK (nitrogen, phosphorus, potassium) in swampy soil.

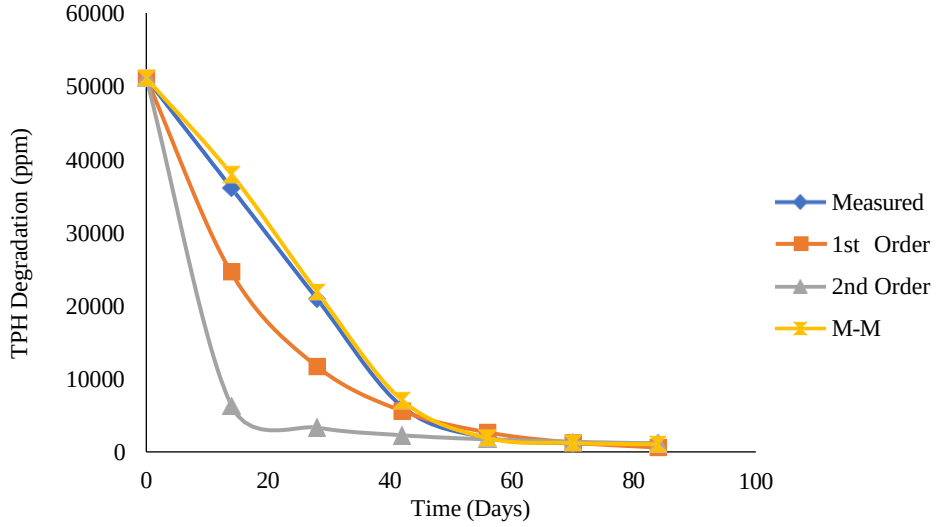

Figure 6. Comparison of models with 100 g moringa seed shell in powdered form, yeast, and NPK (nitrogen, phosphorus, potassium) in swampy soil.

Figures 2–6 show the comparison of the first-order, second-order, and Michaelis-Menten model with values obtained from the experiment at 20 g, 40 g, 60 g, 80 g, and 100 g of moringa seed shell in swampy soil, respectively. From the results obtained from the analysis, the degree of TPH degradation prediction in swampy soil with moringa seed shell treatment cannot be easily distinguished between the Michalis-Menten rate model and the first-order degradation rate model. This is due to the fact that at some point in time, the correlation coefficient (R^2) was higher with the first order, while at other times the Michaelis-Menten model predicted the values of TPH better (see Figures 2–6). This cannot be said for the second-order kinetics as R^2 values in all cases were lower than the two models. Thus, the higher the value of R^2, the more the prediction is closer to the exact experimental value. The measured and the predicted TPH values by the first-order rate, second-order rate, and Michaelis-Menten rate on the 84th day with the respective weights of moringa seed shell for swampy soil are given in Table 1.

Table 1. Comparison of correlation coefficient and predicted total petroleum hydrocarbons (TPH) at 84 days.

Weight (g)	R^2			Measured (ppm)	Predicted (ppm)		
	1st Order	*2nd Order*	*M-M*		*1st Order*	*2nd Order*	*M-M*
20	0.9339	0.9160	0.9739	20026.10	18794.28	18803.41	19748.72
40	0.9372	0.8220	0.9812	9205.35	9678.94	9654.20	8979.98
60	0.9729	0.8351	0.9748	4886.76	4621.66	5331.01	5168.74
80	0.9853	0.8877	0.9639	3041.92	2524.27	2812.29	2099.13
100	0.9527	0.8761	0.9949	1134.35	610.40	1163.36	1041.32

M-M, Michaelis-Menten rate model.

CONCLUSION

The 20 g and 40 g treatment alternatives and the control sample did not, however, differ significantly from one another. Since the TPH in this environment naturally degraded, the control sample frequently performs the worst. As a result, the hydrocarbon-degrading bacteria were unable to attack the substrate because there was no available supply of nutrients for them to draw energy from. soil that has been contaminated by crude oil will undergo bioremediation more quickly if the proper amount of treatment is applied.

Although the best TPH degradation efficiency across all treatment options was reported at the 84th day of analysis, this study demonstrated that increasing the amount of treatment in polluted soil will also raise the percentage that would be eradicated from the soil over time. Although applying 60 g weights of treatment would more economically reduce the cost of receiving the treatment, the treatment would work best when applied between 60 g and 100 g. But there was no appreciable difference between the 20 g and 40 g treatment alternatives and the control sample.

REFERENCES

1. Achinike W, Ekperi NI, Achinike OW. Model comparison of corrosion rate on saline and fresh water environments. Discovery. 2023; 59: e6d1009.
2. Dias RL, Ruberto L, Calabro A, Balbo AL, Del Panno MT, MacCormack WP. Hydrocarbon removal and bacterial community structure in on-site biostimulated biopile systems designed for bioremediation of diesel-contaminated Antarctic soil. Polar Biol. 2015; 38: 677–687.
3. Diele F, Notarnicola F, Sgura I. Uniform air velocity field for a bioventing system design: some numerical results. Int J Eng Sci. 2002; 40: 1199–1210.
4. Dorado AD, Dumont E, Muñoz R, Quijano G. A novel mathematical approach for the understanding and optimization of two-phase partitioning bioreactors devoted to air pollution control. Chem Eng J. 2015; 263: 239–248.
5. Elektorowicz M. Bioremediation of petroleum-contaminated clayey soil with pretreatment. J Environ Technol. 1994; 15: 373–380.

6. Rayner JL, Snape I, Walworth JL, Harvey PM, Ferguson SH. Petroleum–hydrocarbon contamination and remediation by microbioventing at sub-Antarctic Macquarie Island. Cold Register Sci Technol. 2007; 48: 139–153.
7. Reddy KR. Engineering Properties of Soils Based on Laboratory Testing. Chicago, IL: Department of Civil and Material Engineering, University of Illinois, Chicago; 2002.
8. Robles-González IV, Fava F, Poggi-Varaldo HM. A review on slurry bioreactors for bioremediation of soils and sediments. Microb Cell Factories. 2008; 7 (1): 1–7.
9. Rocha C, Infante C. Enhanced oily sludge biodegradation by a tensio-active agent isolated from *Pseudomonas aeruginosa* USBCS1. Appl Environ Microbiol. 1997; 47: 615–619.
10. Ukpaka CP. Development of model for bioremediation of crude oil using moringa seed shell in powdered form, yeast and NPK in swampy soil extract. Chem Int. 2016; 2 (1): 19–28.

